Structures and photoelectron spectroscopy of $Cu_n(BO_2)_m^-$ ($n, m = 1, 2$) clusters: Observation of hyperhalogen behavior

Yuan Feng,[1] Hong-Guang Xu,[1] Weijun Zheng,[1,a)] Hongmin Zhao,[2] Anil K. Kandalam,[3,a)] and Puru Jena[4,a)]

[1]*Beijing National Laboratory for Molecular Sciences, State Key Laboratory of Molecular Reaction Dynamics, Institute of Chemistry, Chinese Academy of sciences, Beijing 100190, China*
[2]*Department of Physics, Beijing Jiaotong University, Beijing 100044, China*
[3]*Department of Physics, McNeese State University, Lake Charles, Louisiana 70609, USA*
[4]*Department of Physics, Virginia Commonwealth University, Richmond, Virginia 23284, USA*

(Received 30 October 2010; accepted 31 January 2011; published online 3 March 2011)

The electronic structures of $CuBO_2^-$, $Cu(BO_2)_2^-$, $Cu_2(BO_2)^-$, and $Cu_2(BO_2)_2^-$ clusters were investigated using photoelectron spectroscopy. The measured vertical and adiabatic detachment energies of these clusters revealed unusual properties of $Cu(BO_2)_2$ cluster. With an electron affinity of 5.07 eV which is larger than that of its BO_2 superhalogen (4.46 eV) building-block, $Cu(BO_2)_2$ can be classified as a hyperhalogen. Density functional theory based calculations were carried out to identify the ground state geometries and study the electronic structures of these clusters. $Cu(BO_2)$ and $Cu(BO_2)_2$ clusters were found to form chainlike structures in both neutral and anionic forms. $Cu_2(BO_2)$ and $Cu_2(BO_2)_2$ clusters, on the other hand, preferred a chainlike structure in the anionic form but a closed ringlike structure in the neutral form. Equally important, substantial differences between adiabatic detachment energies and electron affinities were found, demonstrating that correct interpretation of the experimental photoelectron spectroscopy data requires theoretical support not only in determining the ground state geometry of neutral and anionic clusters, but also in identifying their low lying isomers. © *2011 American Institute of Physics*. [doi:10.1063/1.3556818]

I. INTRODUCTION

Negative ions play an important role in chemistry, as they are the ingredients of all salts. While most of the atoms in the periodic table gain energy in attaching an electron, the halogen atoms, due to the $ns^2\ np^5$ atomic configuration, possess the highest electron affinities (EA) (e.g., Fluorine: 3.40 eV and Chlorine: 3.62 eV (Refs. 1 and 2). Nearly half a century ago it was found that the EA of some polyatomic systems may exceed the 3.62 eV limit.[3] Gutsev and Boldyrev[4] later termed these systems "superhalogens" and proposed a simple formula of $MX_{(n+1)/m}$ to describe them. Here M is a central metal atom and X is an electronegative atom (such as oxygen and halogens). The number of X atoms needed to yield the superhalogen behavior depends upon n, the maximum formal valence of the metal atom, as well as m, the valence of X. Boldyrev and co-workers further established this idea of superhalogens through a series of theoretical studies[5–9] containing *sp*-metal atoms at the center. One of the current authors has reported the superhalogen behavior of BF_4 and AlF_4 clusters.[10] On the experimental front, the smallest gas-phase superhalogens, MX_2 (M = Li and Na; X = Cl, Br, and I) were produced in 1999 by Wang *et al.* and analyzed using photoelectron spectroscopy and theoretical calculations.[11] In the same year, a transition metal based superhalogen, namely MnO_4 was reported in a combined experimental and theoretical study.[12] The past decade has witnessed a significant upsurge in the study of superhalogens and numerous anions such as CrO_4^- (Ref. 13), MX_3^- (M = Mn, Fe, Co, and Ni; X = Cl and Br),[14] $Ta_3F_{16}^-$ (Ref. 15), $Na_xCl_y^-$ (Ref. 16), MX_3^- (M = Be, Mg, and Ca; X = Halogen),[17] $Mg_2F_5^-$ (Ref. 18), MCl_4^- (M = Sc, Y, and La),[19] $Mg_xCl_y^-$ (Ref. 20), and MF_n (M = Cu, Ag, and Au; n = 1–6) (Ref. 21) have been reported.

Recently, BO_2 molecule was also shown to be a superhalogen with an EA of 4.46 eV. Furthermore, its corresponding anion is very stable as it is isoelectronic with CO_2.[22] In a recent joint experimental and computational study,[23] it was reported that gold clusters (Au_n, n = 1–5), when interacted with BO_2 molecule, not only retain their structural identity, but also some of the resulting $Au_n(BO_2)$ clusters were found to exhibit superhalogen behavior. In addition, $[Au_n(BO_2)]^-$ clusters also showed unusual stability which was reflected as high intense peaks in the mass spectra. Similar work[24] involving $Fe_n(BO_2)^-$ clusters, however, revealed very different results. Although the BO_2 moiety retained its structural integrity, in contrast to their gold-counterparts these clusters were not superhalogens. The maximum EA of these clusters was found to be only 2.14 eV for $Fe_6(BO_2)$.

Very recently, a new class of electronegative species called *hyperhalogens* was proposed by two of the current authors.[25] Based upon density functional calculations it was proposed that a new class of electronegative species can be synthesized by surrounding a central metal atom with superhalogen moieties instead of halogen atoms, e.g., Au atom decorated with BO_2 moieties. The electron affinities of these hyperhalogens were shown to be larger than that of their superhalogen building blocks. This hypothesis was

a)Authors to whom correspondence should be addressed. Electronic addresses: zhengwj@iccas.ac.cn, akandalam@mcneese.edu, and pjena@vcu.edu.

verified by carrying out simultaneous experiments using photoelectron spectroscopy. For example, it was shown[25] that $Au(BO_2)_2$ cluster has an EA of 5.7 eV, which is larger than that of BO_2. The fact that hyperhalogens are ternary species provides a greater degree of freedom to design and synthesize new electronegative species than superhalogens, which are composed mostly of binary elements.

A recent systematic study of coinage metal atoms (Cu, Ag, and Au) interacting with F atoms has shown that Cu and Ag atoms can also be used to form superhalogens.[21] We, therefore, wondered if Cu atoms can also form the seed for hyperhalogens. In this article, we report a combined experimental and theoretical study of $Cu_n(BO_2)_m^-$ (n, $m = 1, 2$) clusters. Based on anion photoelectron spectroscopy and density functional theory (DFT) calculations, we show that $Cu(BO_2)_2$ cluster, similar to that of its gold-counterpart, is indeed a hyperhalogen with an adiabatic detachment energy (ADE) of 5.07 eV. However, the $Cu_2(BO_2)$ cluster, unlike $Au_2(BO_2)$ cluster, is *not* a superhalogen. In addition, the ADE and vertical electron detachment energy (VDE) values of $Cu_n(BO_2)_m$ clusters are consistently lower than that of their corresponding $Au_n(BO_2)_m$ counterparts.

II. METHODOLOGIES

A. Experimental method

Experiments were conducted on a home-built apparatus consisting of a time-of-flight mass spectrometer and a magnetic-bottle photoelectron spectrometer, which have been described elsewhere.[26] Briefly, the $CuBO_2^-$, $Cu(BO_2)_2^-$, $Cu_2(BO_2)^-$, and $Cu_2(BO_2)_2^-$ cluster anions were produced in a laser vaporization source by ablating a rotating, translating Cu/B alloy target (13 mm diameter, Cu/B mole ratio 50:1) with the second harmonic (532 nm) light pulses of a Nd:YAG laser, while helium gas with 4 atm backing pressure was allowed to expand through a pulsed valve over the alloy target. The typical laser power used in this work was ~10 mJ/pulse. The residual oxygen on the target surface was sufficient to produce abundant $CuBO_2^-$, $Cu(BO_2)_2^-$, $Cu_2(BO_2)^-$, and $Cu_2(BO_2)_2^-$ clusters, so no additional oxygen was introduced into the source. The cluster anions were mass-analyzed by the time-of-flight mass spectrometer. The $CuBO_2^-$, $Cu(BO_2)_2^-$, $Cu_2(BO_2)^-$, and $Cu_2(BO_2)_2^-$ clusters were each mass-selected and decelerated before being photodetached. The photodetachment of these anions was performed with 266(4.661 eV) and 193 nm (6.424 eV) photons (0.1–0.2 mJ/pulse). The resulting electrons were energy-analyzed by the magnetic-bottle photoelectron spectrometer. The PES spectra were calibrated using the known spectrum of Cu^-. The instrumental resolution was ~40 meV for electrons with 1 eV kinetic energy.

B. Computational method

DFT based calculations were carried out on neutral and negatively charged $Cu_n(BO_2)_m$ clusters using GAUSSIAN 03 (Ref. 27) program. We employed Becke's three parameter hybrid exchange functional[28] with Lee, Yang, and Parr correlation functional[29] (B3LYP) form. An all electron 6–311++G(3*df*) basis sets for B and O atoms, and Lanl2dz basis set for Cu atoms were used during the optimization calculations. The ground state geometries of the anionic and neutral species were determined by optimizing various structural configurations and spin-multiplicities without any symmetry constraints. In the geometry optimization procedure, the convergence criterion was set to 10^{-9} hartree for energy and 10^{-4} hartree/Å for the gradient. The stability of these clusters was confirmed by analyzing their normal mode frequencies. The reliability and accuracy of the functional form and the all electron basis set used in this study has been established by our previous works on $Au_n(BO_2)_m$ clusters.[23,25]

The VDE was calculated as the energy difference between the neutral and anion clusters, both calculated at the ground state geometry of the anion. The EA is defined as the energy difference between the ground state of the anion and the ground state of the neutral clusters. In cases where the geometry of the ground states of the anion and neutral are very different, it may be difficult for the anion to return to the neutral ground state geometry following electron detachment. In this scenario, one has to calculate the ADE. The ADE is obtained by optimizing the geometry of the neutral with the ground state geometry of the anion as a starting point. While it is not possible to identify the geometries of the clusters from the photoelectron spectroscopy studies alone, a comparison of the calculated VDE, ADE, and EA with the experimental photoelectron spectra provides a wealth of information on cluster structure and dynamics.

III. RESULTS AND DISCUSSION

A. Experimental results

A typical mass spectrum obtained in our experiments is shown in Fig. 1. The dominant mass peaks correspond to those of $[Cu_n(BO_2)_m]^-$ cluster anions. Due to the isotopic distributions of copper and boron, these peaks are relatively complex. The assignments of the mass peaks were confirmed by analyzing the isotope abundances of copper–boron dioxide cluster anions. In addition to the $Cu_n(BO_2)_m^-$ series, we also

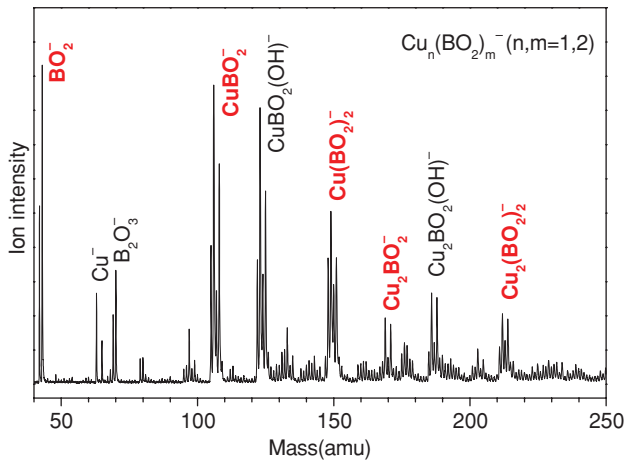

FIG. 1. Mass spectrum of $[CuBO_2]^-$, $[Cu_2(BO_2)]^-$, $[Cu(BO_2)_2]^-$, and $[Cu_2(BO_2)_2]^-$ cluster anions.

observed $Cu_nBO_2(OH)^-$ cluster anions, which are probably due to the residual water in the source.

Interestingly, in the $Cu_n(BO_2)_m^-$ series, the $[CuBO_2]^-$ ion intensity is significantly strong. The intensities of larger clusters drop to a low level and the large cluster anions with mass number higher than 250 amu were not observed in our experiment. These observations may be understood in terms of valence electronic structures. BO_2 is one electron short of electronic shell-closing, so the neutral $CuBO_2$ cluster is a closed-shell species. Thus, other atoms do not add easily to $CuBO_2$. Consequently, the intensities of the larger cluster anions are too low to be detected.

The measured PES spectra of $CuBO_2^-$, $Cu_2(BO_2)^-$, $Cu(BO_2)_2^-$, and $Cu_2(BO_2)_2^-$ are shown in Fig. 2. Each of

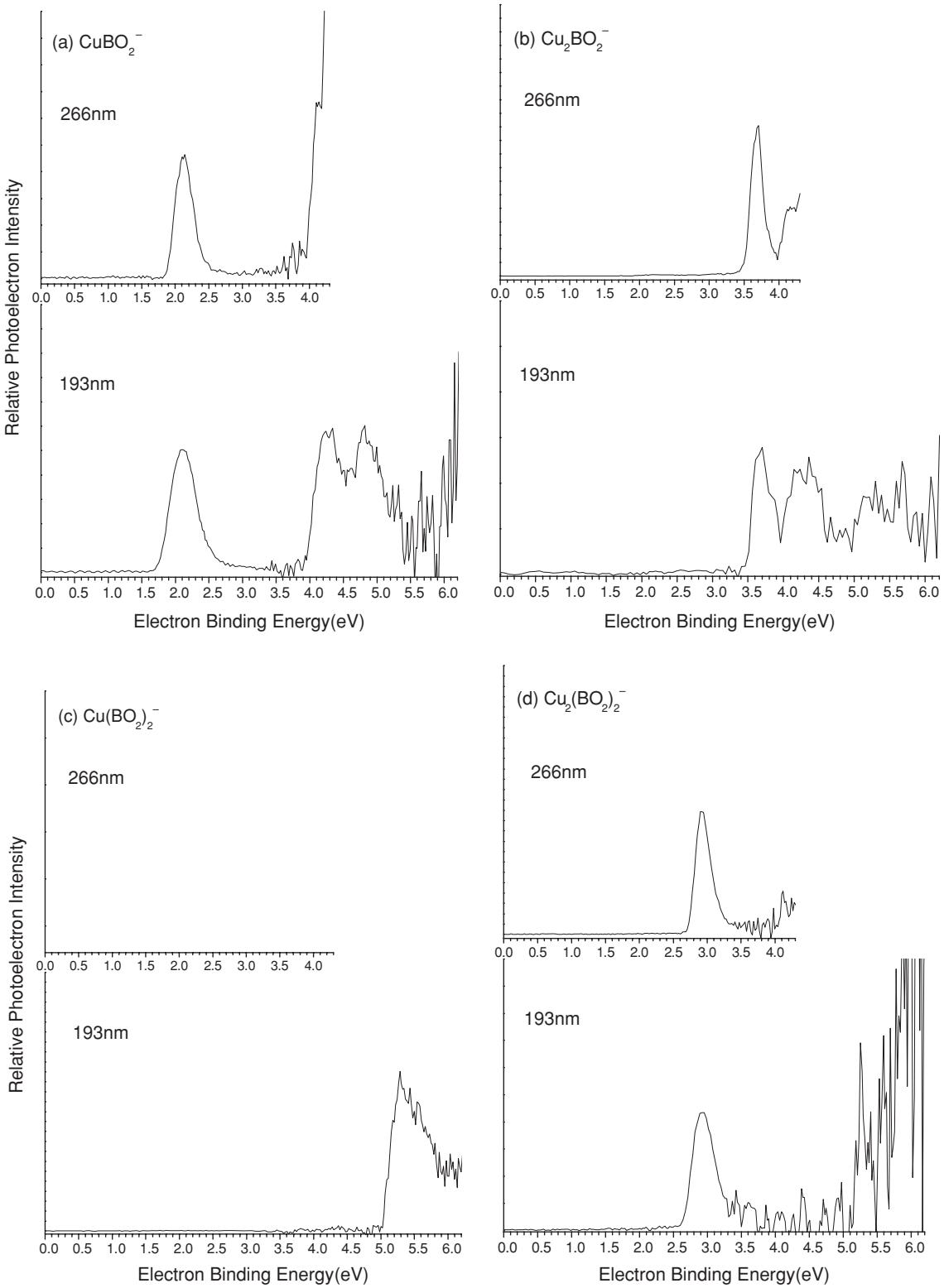

FIG. 2. Photoelectron spectra of $[CuBO_2]^-$, $[Cu_2(BO_2)]^-$, $[Cu(BO_2)_2]^-$, and $[Cu_2(BO_2)_2]^-$ clusters recorded with 266 and 193 nm photons.

TABLE I. Experimental and theoretical ADE and VDE values of $[Cu_n(BO_2)_m]^-$ clusters. The experimental uncertainty is ±0.08 eV.

	ADE (eV)		VDE (eV)	
Clusters	Theory	Expt.	Theory	Expt.
$[CuBO_2]^-$	2.04	1.90	2.17	2.12
$[Cu_2(BO_2)]^-$	3.44	3.53	3.68	3.70
$[Cu(BO_2)_2]^-$	5.31	5.07	5.41	5.28
$[Cu_2(BO_2)_2]^-$	2.97	2.74	3.17	2.92

these PES spectra represents the transitions from the ground state of the anion to the ground or excited states of their corresponding neutral. The VDEs and the ADEs of the cluster anions are estimated from their photoelectron spectra. These values along with their corresponding calculated values are listed in Table I. To account for the broadening of the PES spectrum due to instrumental resolution, the ADE was calculated by adding the half value of instrumental resolution to the onset of the first peak in the spectrum. The onset of the first peak was found by drawing a straight line along the leading edge of that peak towards the baseline of the spectrum. It is normally assumed that the ADE of the cluster anion is equal to the EA of the corresponding neutral. However, we will show later that for some of these clusters ADE and EA are indeed very different.

The PES spectrum of $[CuBO_2]^-$ taken with 193 nm photons [Fig. 2(a), 193 nm] displays a strong peak centered at 2.12 eV, followed by two more features centered at about 4.21 and 4.79 eV. The ADE and VDE of $CuBO_2^-$ are estimated to be 1.90 and 2.12 eV, respectively. Considering the generalizations of Koopmans' theorem, the first and second peak in the spectrum corresponds to the HOMO and LUMO of neutral $CuBO_2$, respectively. Thus, the HOMO–LUMO gap is the energy gap between the first two peaks in the photoelectron spectrum. We estimate the HOMO–LUMO gap of neutral $CuBO_2$ to be ~2.1 eV.

A strong peak centered at 3.70 eV is evident in the PES spectrum of $[Cu_2BO_2]^-$ [Fig. 2(b), 266 nm]. Two more broad features centered at ~4.3 and 5.2 eV are observed with 193 nm photons. The ADE and VDE of $[Cu_2BO_2]^-$ were estimated to be 3.53 and 3.70 eV, respectively.

The $[Cu(BO_2)_2]^-$ cluster cannot be photodetached with a 266 nm photon because it has a high ADE. In the PES spectrum of $[Cu(BO_2)_2]^-$ [Fig. 2(c), 193 nm], the first peak is observed at 5.28 eV. No other feature is observed because the excited states of neutral $Cu(BO_2)_2$ is beyond 193 nm photon energy. Based on the spectrum, we estimate the ADE and VDE of $[Cu(BO_2)_2]^-$ to be 5.07 and 5.28 eV.

For the $[Cu_2(BO_2)_2]^-$ cluster, a dominating sharp peak has been detected at 2.92 eV [Fig. 2(d)]. The VDE and ADE of $[Cu_2(BO_2)_2]^-$ were determined to be 2.74 and 2.92 eV, respectively. The onset of its second feature is observed at around 5.2 eV. This indicates that the HOMO–LUMO gap of neutral $Cu_2(BO_2)_2$ is larger than 2.3 eV.

The large energy difference between the highest occupied (HOMO) and the lowest unoccupied (LUMO) molecular orbital is a good measure of the chemical inertness of a species. In our experiment, the measured HOMO–LUMO gaps of $CuBO_2$ and $Cu_2(BO_2)_2$ are 2.1 and 2.3 eV, respectively (shown in Fig. 2). The large HOMO–LUMO gaps suggest that $CuBO_2$ and $Cu_2(BO_2)_2$ are nonmetallic and should be chemically stable.

B. Theoretical results and discussion

To analyze the experimental data and to understand how the structure and electronic properties are related we describe in the following the equilibrium geometries of neutral and anionic clusters and their computed electron affinity, adiabatic detachment energies in cases they are different from the electron affinities, and vertical detachment energies. The equilibrium geometries of neutral and anionic $Cu_n(BO_2)_m$ (n, m = 1, 2) clusters are shown in Figs. 3–5, while the frontier MOs of the most stable isomers of the negative species are given in Fig. 6.

1. $Cu(BO_2)$ and $Cu_2(BO_2)$ clusters

We begin with the ground state geometries of anionic and neutral $CuBO_2$ in Figs. 3(a) and 3(b), respectively. For these clusters no higher energy isomers were found. We see that the ground state structures of neutral and anionic $Cu(BO_2)$ clusters are the same except for small differences in the bond lengths. In both the structures, the BO_2 mioety maintains its structural integrity, namely it remains linear. These results are similar to those reported earlier[23,24] for neutral and charged $Au_n(BO_2)$ and $Fe_n(BO_2)$ clusters. While the neutral $Cu(BO_2)$ cluster is a singlet, the negatively charged $Cu(BO_2)$ prefers doublet spin state. In order to understand the nature of bonding, we have carried out natural bond orbital (NBO) charge analysis of these clusters. The calculated NBO charges show that in the neutral $Cu(BO_2)$ cluster, the Cu atom has a charge of $+0.87e$, indicating a significant charge transfer from Cu to the BO_2 superhalogen unit. Thus, the bonding in $Cu(BO_2)$ cluster is ionic in nature. In case of the $[Cu(BO_2)]^-$ cluster, the majority of the extra electron's charge (89%) was found to be localized over the positively charged Cu atom, leaving it nearly neutral. The HOMO of the $[CuBO_2]^-$ cluster anion, shown in Fig. 6 indicates that the extra electron mainly localizes on the Cu atom. This is consistent with the NBO analysis. On a comparative note, the charge transfer ($-0.87e$) from Cu to BO_2 in the neutral $Cu(BO_2)$ cluster is larger than the charge transfer ($-0.68e$) from Au atom to BO_2 in our previously reported[23] $Au(BO_2)$ study. This can be understood from the fact that Au is more electronegative than Cu. In fact, the bonding in $Cu(BO_2)$ can be considered as primarily ionic in nature, while in the case of $Au(BO_2)$ cluster the bonding is partially covalent. The calculated VDE of $[Cu(BO_2)]^-$ and the EA of $Cu(BO_2)$ cluster is found to be 2.17 and 2.04 eV, respectively (see Table I). Our calculated values are in good agreement with the measured VDE of 2.12 eV and ADE of 1.90 eV. The identical geometries of neutral and anionic clusters indicate that the measured ADE is indeed the EA of the neutral $Cu(BO_2)$ cluster.

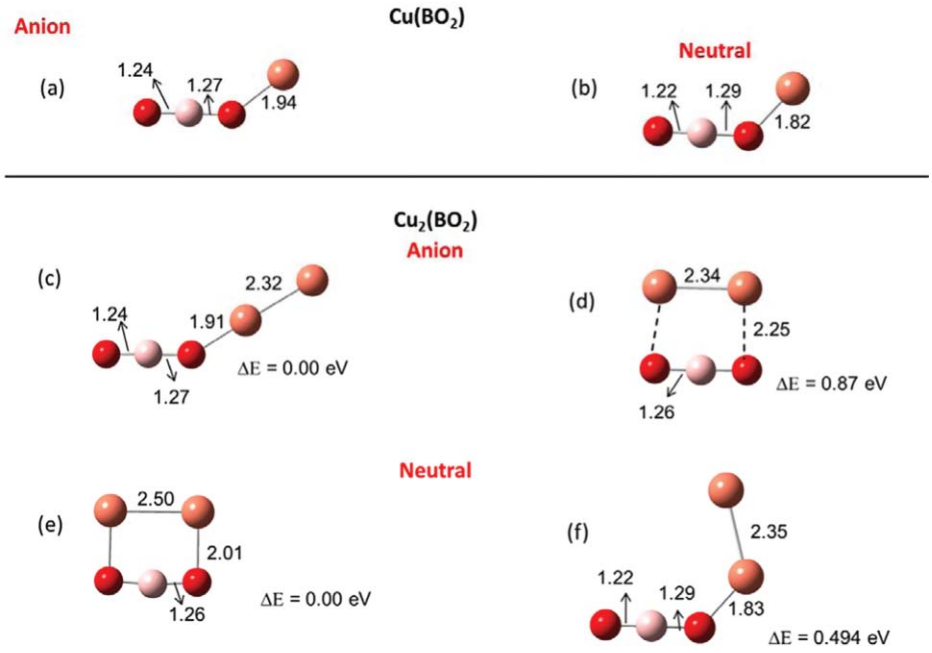

FIG. 3. The geometries of negatively charged and neutral $Cu(BO_2)$ and $Cu_2(BO_2)$ clusters. The relative energies are also given.

The most stable isomer of $[Cu_2(BO_2)]^-$ cluster is in singlet state and has a C_s symmetric bent structure [Fig. 3(c)] with the second Cu atom bind to the first Cu atom. This bent structure is similar to the ground state structure of the previously reported $[Au_2(BO_2)]^-$ and $[Fe_2(BO_2)]^-$ clusters.[23,24] A rectangular ring structure where a Cu_2 unit is interacting with both the oxygen atoms of the BO_2 moiety [Fig. 3(d)] was found to be 0.87 eV higher in energy. A linear isomer ($D_{\infty h}$), in which the Cu atoms occupy the terminal positions (not shown in the figure) was found to be 1.58 eV higher in energy and had a triplet spin multiplicity. The ground state geometry of the neutral $Cu_2(BO_2)$ cluster [see Fig. 3(e)], unlike the anionic $Cu_2(BO_2)$, is not a bent structure, but is identical to the higher energy isomer [Fig. 3(d)] of the anion cluster. On the other hand, the higher energy isomer of the neutral $Cu_2(BO_2)$ cluster [Fig. 3(f)], is similar to the ground state of the anion and lies 0.49 eV higher in energy. Both the neutral isomers prefer a doublet spin state. The geometries where Cu

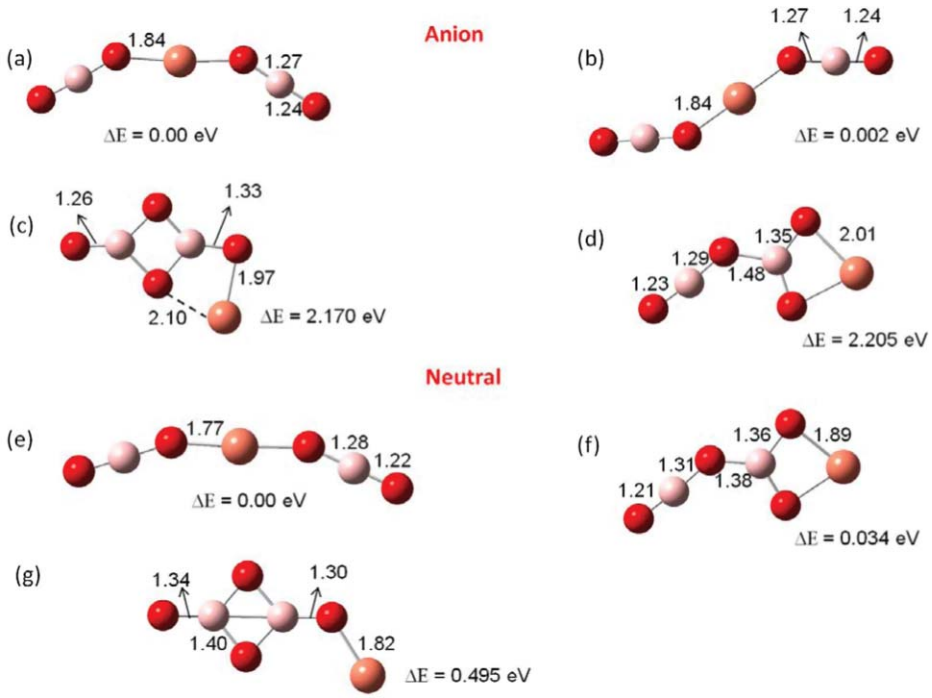

FIG. 4. The ground state geometry and the higher energy isomers of negatively charged and neutral $Cu(BO_2)_2$ cluster.

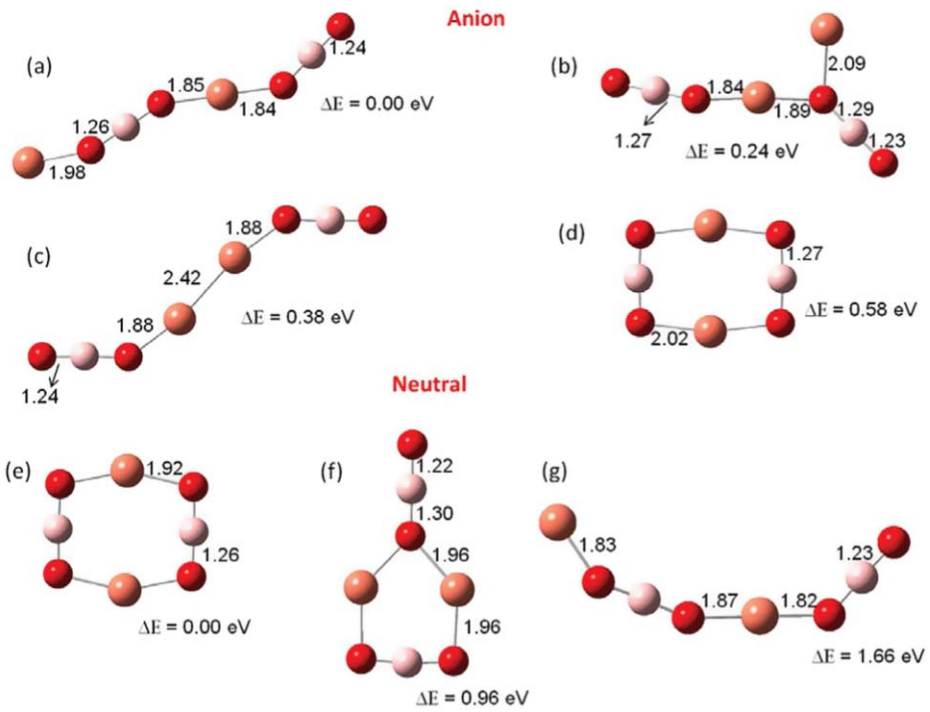

FIG. 5. The ground state and higher energy isomers of negatively charged and neutral $Cu_2(BO_2)_2$ cluster.

atoms do not form a dimer were found to be very high in energy indicating the preference for formation of Cu_2 unit when interacting with a single BO_2 molecule.

A comparison of the NBO charges of Cu_2 unit in negatively charged and neutral $Cu_2(BO_2)$ cluster shows that the Cu_2 unit loses 87% of the charge during the photodetachment process. The HOMO of $[Cu_2(BO_2)]^-$ cluster (shown in Fig. 6) corresponds to the non-bonding orbital on the two Cu atoms and is consistent with the NBO analysis that the VDE is due to the electron detachment from the Cu_2 unit. The calculated

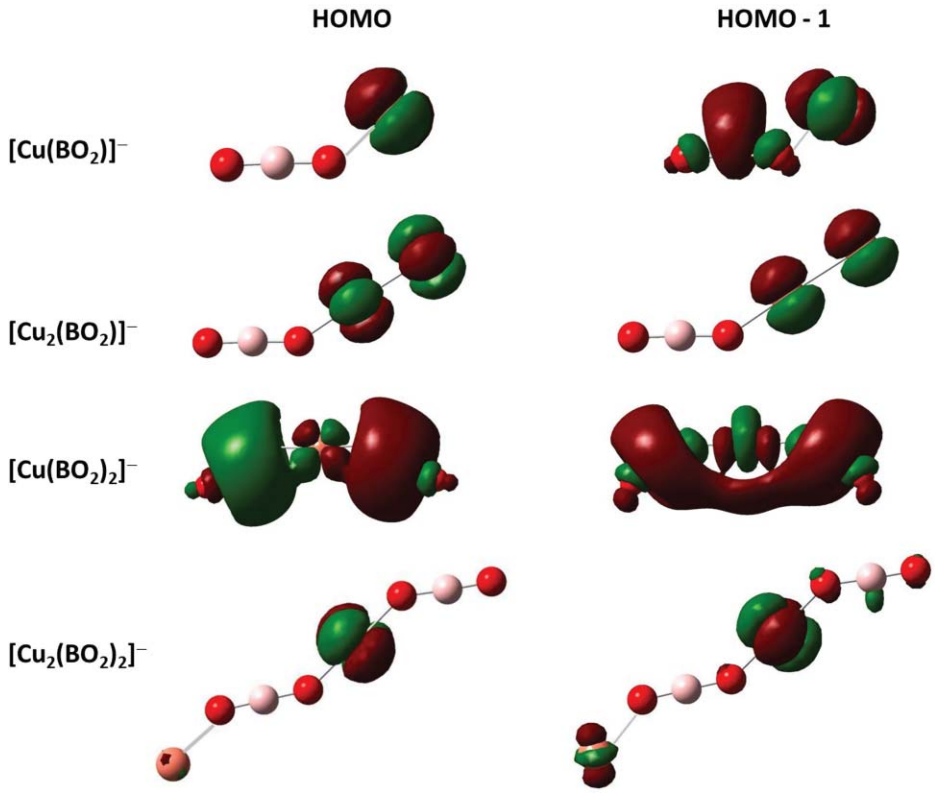

FIG. 6. The frontier molecular orbitals of the most stable isomers of $[Cu_n(BO_2)_m]^-$ (n, $m = 1, 2$) clusters.

VDE of $[Cu_2(BO_2)]^-$ cluster is 3.68 eV and is in excellent agreement with the measured VDE of 3.70 eV. On the other hand, our calculated EA of 2.95 eV does not match with the experimental ADE value of 3.53 eV. This is to be expected since the anionic ground state and neutral ground state geometries of $Cu_2(BO_2)$ clusters are different. As the electron is photodetached from the anion, it will first relax to its nearest local minimum with geometry close to the anion. Our computed ADE, which is the energy difference between the ground state anion [Fig. 3(c)] and the higher energy neutral isomer at similar geometry as the anion [Fig. 3(f)], is found to be 3.44 eV. This is in good agreement with the experimental threshold/onset energy of 3.53 eV. In addition, the energy barrier between the ground state neutral (3(e)) and the higher energy (3(f)) isomer was calculated to be 0.503 eV, thus avoiding the conversion into neutral ground state isomer. This shows unambiguously that the measured ADE of $[Cu_2(BO_2)]^-$ is *not* equal to the EA of neutral $Cu_2(BO_2)$ cluster.

It is to be further noted here that the VDE and ADE values of $[Cu(BO_2)]^-$ and $[Cu_2(BO_2)]^-$ clusters are significantly smaller than those of the corresponding values of $[Au(BO_2)]^-$ and $[Au_2(BO_2)]^-$ clusters.[23] For example, the calculated ADE and VDE values of $[Au_2(BO_2)]^-$ clusters were 4.66 and 4.80 eV, respectively. Thus, while $Au_2(BO_2)$ cluster is a superhalogen, $Cu_2(BO_2)$ cluster is not. This demonstrates the uniqueness of gold among the coinage-metal atoms. The significant difference in the ADE and VDE values of $Au_n(BO_2)$ and $Cu_n(BO_2)$ clusters is due to the enhanced ability of Au atoms to accommodate the extra electron as compared to the Cu atoms.

2. $Cu(BO_2)_2$ and $Cu_2(BO_2)_2$ clusters

We now turn to the structures and energetics of neutral and anionic $Cu(BO_2)_2$ and $Cu_2(BO_2)_2$ clusters. The most stable and higher energy isomers of neutral and negatively charged $Cu(BO_2)_2$ cluster are given in Fig. 4. The ground state geometry of $[Cu(BO_2)_2]^-$ cluster is a *cis* structure (C_{2v} symmetry) with a central Cu atom bound to two BO_2 superhalogen moieties on either side [Fig. 4(a)]. The corresponding *trans* configuration [Fig. 4(b)] is energetically degenerate ($\Delta E = 0.002$ eV) with the ground state geometry. On the other hand, the structural configurations containing B_2O_4 units [Figs. 4(c) and 4(d)] were found to be higher in energy ($\Delta E > 2.0$ eV). The energy barrier between the *cis* and *trans* configurations is calculated to be less than 0.024 eV, which is smaller than the uncertainty of our computational procedure. The $[Cu(BO_2)_2]^-$ cluster is a closed-shell system with singlet spin. The ground state geometry of the neutral $Cu(BO_2)_2$ cluster [Fig. 4(e)] has a doublet spin multiplicity and is nearly identical to its anionic counterpart [Fig. 4(a)]. Interestingly, the structure containing B_2O_4 unit [Fig. 4(f)], is found to be energetically degenerate ($\Delta E = 0.03$ eV) with the neutral ground state structure. It is noteworthy here that the ground state geometries of anionic and neutral $Cu(BO_2)_2$ clusters are identical to the corresponding $Au(BO_2)_2$ cluster.[25] In addition, the stabilization of B_2O_4 unit-containing structure in the neutral species was also observed in the $Au(BO_2)_2$ cluster.

The most interesting feature of $Cu(BO_2)_2$ cluster, however, is its electron affinity. The calculated VDE and ADE of $[Cu(BO_2)_2]^-$ cluster are 5.41 and 5.31 eV, respectively and are in good agreement with the experiment values. Since, the ground state geometries of neutral and anionic $Cu(BO_2)_2$ clusters are nearly identical, our calculated ADE of the anion corresponds to the EA of the neutral cluster. Thus, the calculated EA of $Cu(BO_2)_2$ is 5.31 eV, which is the largest EA of any of the $Cu_n(BO_2)_m$ clusters in the present study. Since $Cu(BO_2)_2$ consists of a central metal atom bonded to BO_2 superhalogen moieties and its EA is larger than that of its superhalogen building units (EA of $BO_2 = 4.46$ eV), we term $Cu(BO_2)_2$ cluster as a hyperhalogen. This has been described in our previous publication.[25]

The origin of the unusually large EA value of $Cu(BO_2)_2$ and the large VDE of $[Cu(BO_2)_2]^-$ cluster can be understood from the NBO charge analysis. In the case of neutral $Cu(BO_2)_2$ cluster, the Cu atom has charge of $+1.38e$, while each of the BO_2 units have a charge of $-0.69e$, indicating the ionic nature of bonding between the Cu atom and the BO_2 moieties. On the other hand, the NBO charge analysis of $[Cu(BO_2)_2]^-$ cluster showed that the extra electron is delocalized over the entire cluster, with 58% on the Cu atom and 42% on the two BO_2 units. The delocalization of the extra electron over the entire cluster rather than localizing on just the Cu atom is responsible for the unusually large EA value of $Cu(BO_2)_2$ cluster. The delocalization of the extra-electron's charge over the entire cluster can also be seen in the HOMO of $[Cu(BO_2)_2]^-$ cluster (Fig. 6). We now compare the EA values of CuX_2 (X = F, Cl, Br, and I) molecules with that of the $Cu(BO_2)_2$ cluster. The EA of CuF_2 molecule was reported[21] to be 3.79 eV, while our calculations of CuX_2 (X = Cl, Br, and I) molecules show that they are superhalogens with EA values of 4.41, 4.35, and 4.22 eV, corresponding to $CuCl_2$, $CuBr_2$, and CuI_2, respectively. Our calculated EA values are in good agreement with the previously reported photoelectron spectroscopy and theoretical investigation[30] of $CuCl_2^-$ and $CuBr_2^-$ clusters. We are not aware of any measured EA values of CuI_2 cluster. Thus, the EAs of CuX_2 species are consistently smaller, by a significant amount, than the EA of $Cu(BO_2)_2$ cluster. Thus, the concept of hyperhalogens where the halogen atoms around a central metal atom are replaced with superhalogen moieties to enhance the EA of the resulting species is valid for $Cu(BO_2)_2$ as it was for $Au(BO_2)_2$ cluster.

We now turn to the largest cluster in the present study, namely, $Cu_2(BO_2)_2$ cluster. The ground state geometry and the higher energy isomers of neutral and negatively charged $Cu_2(BO_2)_2$ cluster are given in Fig. 5. The ground state geometry of $[Cu_2(BO_2)_2]^-$ is a long chainlike structure [Fig. 5(a)] which can be obtained by adding a Cu atom to the *trans*-form of $[Cu(BO_2)_2]^-$ cluster [Fig. 4(b). One can also visualize this structure as two units of $Cu(BO_2)$ clusters bonded together with Cu–O bonds in the center. Interestingly, the chain isomer containing a central Cu_2 unit with the two BO_2 moieties bonded on either side of the metal dimer [Fig. 5(c)] was found to be 0.38 eV higher in energy. The isomer in Fig. 5(b) with each Cu atom forming bonds with O was found to be 0.24 eV higher in energy than the ground state structure.

An eight membered ring structure, with two O–Cu–O bonds [Fig. 5(d)] was found to be 0.58 eV higher in energy. Thus, in the case of negatively charged $Cu_2(BO_2)_2$, unlike in the $Cu_2(BO_2)$, the Cu–Cu bonding is not preferred. The calculated VDE and ADE of the ground state structure are 3.17 and 2.97 eV, which are consistent with the experimental values of 2.92 and 2.74 eV, respectively. The calculated VDEs for the higher energy isomers [Figs. 5(b) and 5(c)] are 3.4 and 5.06 eV, which do not match with the measured values. Therefore, only the ground state structure is present in the cluster beam and is contributing to the PES spectrum.

The ground state geometry of neutral $Cu_2(BO_2)_2$ cluster, unlike its anionic counterpart, is not chainlike, but an eight membered ring structure [Fig. 5(e)]—in analogy with a similar geometry of the higher energy isomer of the anion [Fig. 5(d)]. The geometry similar to that of the anion ground state yielded a higher energy isomer shown in Fig. 5(g). This chainlike structure is 1.66 eV higher in energy than the neutral ground state geometry. Since, the ground state geometries of anion and neutral $Cu_2(BO_2)_2$ clusters are vastly different from each other, the measured ADE value of the $[Cu_2(BO_2)]^-$ does not correspond to the EA of $Cu_2(BO_2)_2$ cluster. In fact, the electron affinity of the $Cu_2(BO_2)_2$ is calculated to be only 1.31 eV.

Based on these results, one can visualize long chainlike structures for larger $[Cu(BO_2)]_n^-(n > 2)$ clusters, while a closed-ringlike structure for the corresponding neutral $[Cu(BO_2)]_n$ clusters. Computational investigations in this direction are currently underway.

IV. CONCLUSIONS

In summary, a synergistic study involving photoelectron spectroscopy and density functional theory calculations have yielded interesting results for the geometries, electronic structure, vertical and adiabatic detachment energies, and electron affinities of $Cu_n(BO_2)_m$ clusters. Based on MO analysis, we found that that the extra electron is localized on the Cu_n units for $[Cu_n(BO_2)]^-$ $(n = 1, 2)$ clusters, while in $[Cu(BO_2)_2]^-$ cluster, the excess electron is delocalized over the entire cluster. For $[Cu_2(BO_2)_2]^-$ cluster, the excess electron is localized on the Cu atom between the two BO_2 units. We note that while some of the Cu-based clusters show similarity with Au-based clusters, significant differences in structures and electron affinities are found. Thus, all coinage metals cannot be assumed to show similar behavior. However, both Cu and Au-based clusters show that the hyperhalogen behavior may be a general occurrence and even higher electron affinities can be achieved by changing the building blocks from halogens to superhalogens. Since hyperhalogens contain three different elements, one has much more freedom in designing a large number of highly electronegative species than superhalogens. Note that the latter only contains two different elements. The possibility of creating new highly electronegative species can give rise to the synthesis of salts with unusual properties.

ACKNOWLEDGMENTS

W.J.Z. acknowledges the Institute of Chemistry, Chinese Academy of Sciences for start-up funds. A.K.K. acknowledges the faculty start-up funds made available through the Louisiana Board of Regents-Research Commercialization/Educational Enhancement Program (RC/EEP). P.J. acknowledges partial support of the Defense Threat Reduction Agency and the (U.S.) Department of Energy (DOE).

[1] H. Hotop and W. C. Lineberger, J. Phys. Chem. Ref. Data **14**, 731 (1985).
[2] U. Berzinsh, M. Gustafsson, D. Hanstorp, A. Klinkmuller, U. Ljungblad, and A. M. Martenssonpendrill, Phys. Rev. A **51**, 231 (1995).
[3] N. Bartlett and D. H. Lohman, Proc. Chem. Soc. 115 (1962); N. Bartlett, Proc. Chem. Soc. 218 (1962).
[4] G. L. Gutsev and A. I. Boldyrev, Chem. Phys. **56**, 277 (1981).
[5] G. L. Gutsev and A. I. Boldyrev, Chem. Phys. Lett. **108**, 250 (1984).
[6] G. L. Gutsev and A. I. Boldyrev, J. Phys. Chem. **94**, 2256 (1990).
[7] A. I. Boldyrev and J. Simons, J. Chem. Phys. **97**, 2826 (1991).
[8] A. I. Boldyrev and W. von Niessen, Chem. Phys. **155**, 71 (1991).
[9] A. I. Boldyrev and J. Simons, J. Chem. Phys. **99**, 4628 (1993).
[10] G. L. Gutsev, P. Jena, and R. J. Bartlett, Chem. Phys. Lett. **292**, 289 (1998).
[11] X.-B. Wang, C.-F. Ding, L.-S. Wang, A. I. Boldyrev, and J. Simons, J. Chem. Phys. **110**, 4763 (1999).
[12] G. L. Gutsev, B. K. Rao, P. Jena, X. B. Wang, and L.-S. Wang, Chem. Phys. Lett. **312**, 598 (1999).
[13] G. L. Gutsev, P. Jena, H.-J. Zhai, and L.-S. Wang, J. Chem. Phys. **115**, 7935 (2001).
[14] X. Yang, X.-B. Wang, L.-S. Wang, S. Niu, and T. Ichiye, J. Chem. Phys. **119**, 8311 (2003).
[15] M. Sobczyk, A. Sawicka, and P. Skurski, Eur. J. Inorg. Chem. **20**, 3790 (2003).
[16] A. N. Alexandrova, A. I. Boldyrev, Y.-J. Fu, X. Yang, X.-B. Wang, and L.-S. Wang, J. Chem. Phys. **121**, 5709 (2004).
[17] B. M. Elliot, E. Koyle, A. I. Boldyrev, X.-B. Wang, and L.-S. Wang, J. Phys. Chem. A **109**, 11560 (2005).
[18] I. Anusiewicz and P. Skurski, Chem. Phys. Lett. **440**, 41 (2007).
[19] J. Yang, X.-B. Wang, X.-P. Xing, and L.-S. Wang, J. Chem. Phys. **128**, 201102 (2008).
[20] I. Anusiewicz, Aust. J. Chem. **61**, 712 (2008).
[21] P. Koirala, M. Willis, B. Kiran, A. K. Kandalam, and P. Jena, J. Phys. Chem. C **114**, 16018 (2010).
[22] H.-J. Zhai, L.-M. Wang, S.-D. Li, and L.-S. Wang, J. Phys. Chem. A **111**, 1030 (2007).
[23] M. Götz, M. Willis, A. K. Kandalam, G. F. Ganteför, and P. Jena, ChemPhysChem **11**, 853 (2010).
[24] Y. Feng, H.-G. Xu, Z.-G. Zhang, Z. Gao, and W. J. Zheng, J. Chem. Phys. **132**, 074308 (2010).
[25] M. Willis, M. Götz, A. K. Kandalam, G. F. Ganteför, and P. Jena, Angew. Chem., Int. Ed. **49**, 8966 (2010).
[26] H.-G. Xu, Z.-G. Zhang, Y. Feng, J.-Y. Yuan, Y.-C. Zhao, and W.-J. Zheng, Chem. Phys. Lett. **487**, 204 (2010).
[27] M. J. Frish, G. W. Trucks, H. B. Schlegel *et al.*, GAUSSIAN 03, Revision D.02. Gaussian, Inc., Wallingford, CT, 2004.
[28] A. D. Becke, J. Chem. Phys. **98**, 5648 (1993).
[29] C. Lee, W. Yang, and R. G. Parr, Phys. Rev. B **37**, 785 (1988).
[30] X.-B. Wang, L.-S. Wang, R. Brown, P. Schwerdtfeger, D. Schroeder, and H. Schwarz, J. Chem. Phys. **114**, 7388 (2001).